

Metal-Dependent and Redox-Selective Coordination Behaviors of Metalloligand $[\text{Mo}^{\text{V}}(1,2\text{-benzenedithiolato})_3]^-$ with $\text{Cu}^{\text{I}}/\text{Ag}^{\text{I}}$ Ions

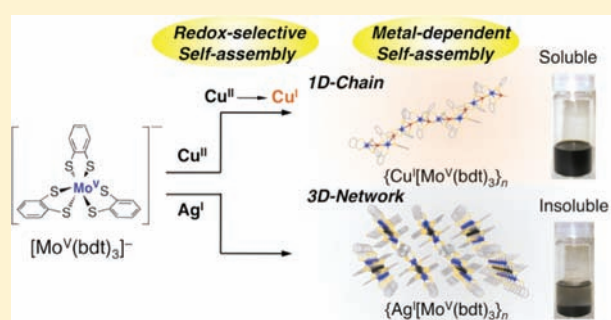
Takeshi Matsumoto,[†] Ho-Chol Chang,^{*,‡} Atsushi Kobayashi,[‡] Kohei Uosaki,^{†,‡,§} and Masako Kato^{*,†,‡}

[†]Center for Strategic Utilization of Elements and [‡]Division of Chemistry, Faculty of Science, Hokkaido University, North-10, West-8, Kita-ku, Sapporo 060-0810, Japan

[§]International Center for Materials Nanoarchitectonics, National Institute for Materials Science (NIMS), 1-1 Namiki, Tsukuba-city, Ibaraki, 305-0044, Japan

S Supporting Information

ABSTRACT: The synthesis and characterization of two coordination polymers, $\{\text{Cu}^{\text{I}}[\text{Mo}^{\text{V}}(\text{bdt})_3] \cdot 0.5\text{Et}_2\text{O}\}_n$ ($1 \cdot 0.5\text{Et}_2\text{O}$, bdt: *o*-benzenedithiolato) and $\{\text{Ag}^{\text{I}}[\text{Mo}^{\text{V}}(\text{bdt})_3]\}_n$ (**2**), composed of redox-active $[\text{Mo}^{\text{V}}(\text{bdt})_3]^-$ metalloligand with Cu^{I} and Ag^{I} ions are reported. The complexation reactions of $[\text{Mo}^{\text{V}}(\text{bdt})_3]^-$ with $\text{Cu}^{\text{II}}(\text{ClO}_4)_2$ or $\text{Ag}^{\text{I}}\text{ClO}_4$ commonly lead to the formation of one-dimensional (1-D) coordination polymers. The presence of Cu^{I} in $1 \cdot 0.5\text{Et}_2\text{O}$ strongly indicates that the Cu^{II} ion is reduced during the complexation reaction with $[\text{Mo}^{\text{V}}(\text{bdt})_3]^-$, which acts as an electron donor. The total dimensionalities of the assembled structures of $1 \cdot 0.5\text{Et}_2\text{O}$ and **2** are significantly different and related to the type of additional metal ions, Cu^{I} and Ag^{I} . In contrast to the isolated 1-D chain structure of $1 \cdot 0.5\text{Et}_2\text{O}$, complex **2** has a three-dimensional (3-D) assembled structure constructed from additional $\pi-\pi$ stacking interactions between adjacent $[\text{Mo}^{\text{V}}(\text{bdt})_3]^-$ moieties. These structural differences influence the solubility of the complexes in organic solvents; complex $1 \cdot 0.5\text{Et}_2\text{O}$ is soluble as oligomeric species in highly polar solvents, while **2** is insoluble in organic solvents and water. Coordination polymers $1 \cdot 0.5\text{Et}_2\text{O}$ and **2** were investigated by UV-vis spectroscopy in the solid state, and that in solution together with their electrochemical properties were also investigated for **1** because of its higher solubility in polar organic solvents. Complex $1 \cdot 0.5\text{Et}_2\text{O}$ dissolved in CH_3CN demonstrates concentration-dependent UV-vis spectra supporting the presence of coordinative interactions between $[\text{Mo}^{\text{V}}(\text{bdt})_3]^-$ moieties and Cu^{I} ions to create the oligomeric species even in solutions, an observation that is supported also by electrochemical experiments.



INTRODUCTION

The design of a molecule-based assembly that shows intriguing structures and properties has attracted increasing attention not only in the field of coordination chemistry but also in supramolecular functional chemistry.¹ To date, several types of supramolecular assemblies have been constructed by utilizing coordination-directed self-assembly of transition metals and functional organic and/or inorganic ligands having specific metal-coordinating sites.² A useful approach in overcoming difficulties in the rational creation of systems with multiple components, together with the difficulty in controlling of their overall structures, is to use metal complexes as metalloligands. A metalloligand can be defined as a complex that contains several potential donor groups that enable coordination to a variety of metal ions, as modules to design and build up assemblies composed of multiple components. Among the well-established metalloligands, interest in the chemistry of dithiolene complexes has increased tremendously in the past five decades since their initial popularity in the 1960s.³ Early interest focused primarily on the structural geometries,⁴ redox properties,⁵ and magnetic

properties⁶ of this class of complexes, which arise from the “non-innocent property”⁷ of dithiolenes. Recently, this interest has expanded, stimulated in part by their potential applications in diverse areas such as light energy conversion schemes,⁸ nonlinear optics,⁹ Q-switch laser dyes, light-driven information devices,¹⁰ as well as their biological relevance as models for molybdenum- and tungsten-based enzymes.¹¹ In particular, tris(*o*-benzenedithiolato)molybdenum complexes $[\text{Mo}(\text{bdt})_3]^n$ ($n = 0, -1$, and -2) form a redox series including neutral, monoanionic, and dianionic species. The coordination geometries of the MoS_6 polyhedron, electro- and photochemical properties, and reactivities of these complexes have been discussed at various levels of sophistication.¹²

From the aspect of the creation of a novel type of metal-based assembly, the $[\text{M}(\text{bdt})_3]^n$ ($n = 0, -1$, and -2) unit should be a fascinating candidate as the metalloligand, which enables study of the electro- and/or photochemical activities. Such an

Received: October 13, 2010

Published: March 09, 2011

Table 1. Crystallographic Data for 1·0.5Et₂O and 2

	1·0.5Et ₂ O	2
formula	C ₂₀ H ₁₇ CuMoO _{0.5} S ₆	C ₁₈ H ₁₂ AgMoS ₆
fw	617.2	624.46
crystal size (mm ³)	0.28 × 0.24 × 0.18	0.36 × 0.08 × 0.04
crystal system	orthorhombic	monoclinic
space group	<i>Pbca</i> (No. 61)	<i>P2₁/n</i> (No. 14)
<i>a</i> (Å)	19.389(3)	12.415(2)
<i>b</i> (Å)	20.128(3)	7.2458(9)
<i>c</i> (Å)	22.311(3)	22.323(3)
β (deg)	90	104.8072(5)
<i>V</i> (Å ³)	8908(2)	1941.3(4)
<i>T</i> (K)	183	223
<i>Z</i>	16	4
<i>D</i> _{calc} (g cm ⁻³)	1.840	2.136
<i>F</i> (000)	4928	1220
μ (Mo K α)(cm ⁻¹)	20.873	22.966
measured reflns.	148734	15339
unique reflns.	13054	4389
refined parameters	515	236
GOF on <i>F</i> ²	1.180	1.099
<i>R</i> _{int}	0.048	0.015
<i>R</i> ₁ ^a	0.0543	0.0227
<i>wR</i> ₂ ^b (all data)	0.1445	0.0567

$$^a R_1 = \sum ||F_o| - |F_c|| / \sum |F_o|, \quad ^b wR_2 = \{ [\sum w(F_o^2 - F_c^2)^2] / [\sum w(F_o^2)^2] \}^{1/2}.$$

investigation of [M(dithiolato)_{*m*}]^{*n*} complexes focusing on their utilization as a metallogand has been limited to only a few examples.¹³ In this paper, the complexation abilities of [Mo^V(bdt)₃]⁻ with Cu^{II}(ClO₄)₂ and Ag^IClO₄ are reported, together with electro- and spectrochemical properties of the two new assemblies.

EXPERIMENTAL SECTION

General Procedures. All synthetic operations and measurements were performed under N₂ atmosphere using Schlenk-line techniques unless otherwise noted. Cu^{II}(ClO₄)₂·6H₂O and Ag^IClO₄ were purchased from Aldrich. Cu^I(CH₃CN)₄ClO₄ was synthesized by the reported procedures.¹⁴ Tetrahydrofuran (THF) was distilled from Na metal under N₂ atmosphere prior to use. The other solvents (diethyl ether (Et₂O), *N,N*-dimethylformamide (DMF), and acetonitrile (CH₃CN)) were used without any purification. *n*-Bu₄N[Mo^V(bdt)₃] and [Mo^{VI}(bdt)₃] were synthesized by the reported procedures.^{12a,b} **Caution!** Although we have experienced no difficulties with the perchlorate salts, these should be regarded as potentially explosive and handled with care.

Physical Measurements. Elemental analyses were performed at the analysis center in Hokkaido University. Electrochemical experiments were performed with a BAS model 650A electrochemical analyzer using a glassy carbon working electrode and a platinum auxiliary electrode. The reference electrode was made from a silver wire inserted into a small glass tube fitted with a porous vycor frit at the tip and filled with a CH₃CN solution containing 0.1 M *n*-Bu₄NClO₄ and 0.01 M AgNO₃. All three electrodes were immersed in a 20 mL CH₃CN solution containing 0.1 M *n*-Bu₄NPF₆ as a support electrolyte and analytes. In all cases, redox potentials are measured with respect to the Ag/Ag⁺ redox couple. Absorption spectra in solution were recorded on a Shimadzu MultiSpec-1500 spectrophotometer over the range 190–800 nm at 296 K. Absorption spectra in the solid state were recorded on a Hitachi

U-3000 spectrophotometer over the range 190–900 nm at 296 K using KBr pellets containing 1, 2, and *n*-Bu₄N[Mo^V(bdt)₃].

Crystallographic Data Collection and Refinement of Structures. The crystallographic measurements were performed using a Rigaku AFC-7R diffractometer with Mercury CCD area detector, graphite monochromated Mo K α radiation ($\lambda = 0.71069$ Å). Specimens of suitable size and quality were selected and mounted onto a glass fiber. The structures were solved by direct methods (SIR2004)¹⁵ and expanded using Fourier techniques (DIRDIF99),¹⁶ which successfully located non-hydrogen atoms. All calculations were performed using the CrystalStructure crystallographic software package¹⁷ except for refinement, which was performed using SHELXL-97.¹⁸ A summary of the crystallographic data for 1·0.5Et₂O and 2 is given in Table 1. Full crystallographic details have been deposited with the Cambridge Crystallographic Data Centre as supplementary publication nos. CCDC-393564 for 1·0.5Et₂O and CCDC-393565 for 2.

Synthesis of {Cu^I[Mo^V(bdt)₃]·0.5Et₂O}_{*n*} (1·0.5Et₂O) from Cu^{II}(ClO₄)₂·6H₂O. A THF (5 mL) solution of Cu^{II}(ClO₄)₂·6H₂O (122 mg, 0.33 mmol) was added to an olive green THF (10 mL) solution of *n*-Bu₄N[Mo^V(bdt)₃] (250 mg, 0.33 mmol) at room temperature (RT). The color of the reaction mixture changed immediately to bright green. After stirring for 24 h, a black precipitate was obtained and collected by filtration. After washing with THF (5 mL × 5) for removal of THF-soluble byproduct, the black powder was dried in vacuo. The product was dissolved in DMF (20 mL) and precipitated by adding Et₂O (20 mL). Filtration of the suspension followed by washing with Et₂O (5 mL × 5), yielded the product as a dark purple powder. Yield 41%. Anal. Calcd for C₂₀H₁₇O_{0.5}S₆MoCu (1·0.5Et₂O): C, 38.92; H, 2.78. Found: C, 38.65; H, 2.57. The complex was recrystallized from DMF/Et₂O to give dark purple crystals suitable for X-ray crystallographic analysis.

Synthesis of {Cu^I[Mo^V(bdt)₃]·0.5Et₂O}_{*n*} (1·0.5Et₂O) from Cu^I(CH₃CN)₄ClO₄. A THF (35 mL) suspension of Cu^I(CH₃CN)₄ClO₄ (70 mg, 0.21 mmol) was added to an olive green THF (10 mL) solution of *n*-Bu₄N[Mo^V(bdt)₃] (150 mg, 0.20 mmol) at RT. The color of the reaction mixture changed to dark brown, and a black precipitate was obtained immediately. After stirring for 4 h, a black precipitate was collected by filtration. After washing with THF (5 mL × 5) for removal of THF-soluble byproduct, the black powder was dried in vacuo. The product was dissolved in DMF (10 mL) and precipitated by adding Et₂O (10 mL). Filtration of the suspension followed by washing with Et₂O (5 mL × 5), yielded the product as a dark purple powder. Yield 81%. The complex was recrystallized from DMF/Et₂O to give dark purple crystals.

Synthesis of {Ag^I[Mo^V(bdt)₃]_{*n*} (2). A THF (5 mL) solution of Ag^IClO₄ (68.3 mg, 0.33 mmol) was added to an olive green THF (10 mL) solution of *n*-Bu₄N[Mo^V(bdt)₃] (250 mg, 0.33 mmol) at RT. The color of the reaction mixture changed immediately to dark green. After stirring for 24 h, a black precipitate was obtained and collected by filtration. After washing with THF (5 mL × 5) for removal of THF-soluble byproduct, the black powder was dried in vacuo. Yield 76%. Anal. Calcd for C₁₈H₁₂S₆MoAg: C, 34.62; H, 1.94. Found: C, 34.76; H, 2.10. Black single crystals suitable for X-ray crystallographic analysis were obtained by layering a CH₃CN solution of Ag^IClO₄ (68.3 mg, 0.33 mmol) onto an acetone solution of *n*-Bu₄N[Mo^V(bdt)₃] (250 mg, 0.33 mmol).

RESULTS AND DISCUSSION

Syntheses of 1·0.5Et₂O and 2. Treatment of the olive green THF solution of *n*-Bu₄N[Mo^V(bdt)₃] with the pale blue THF solution of Cu^{II}(ClO₄)₂·6H₂O at RT for 24 h afforded 1·0.5Et₂O as a black precipitate (Scheme 1). Complex 1·0.5Et₂O was isolated in 41% yield by adding Et₂O to cause reprecipitation from DMF solution. It is a dark purple powder

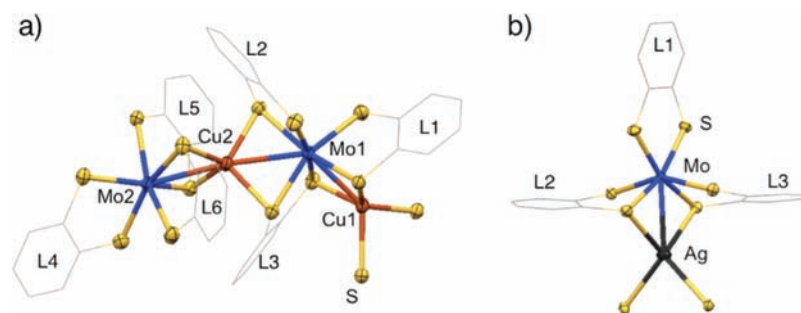
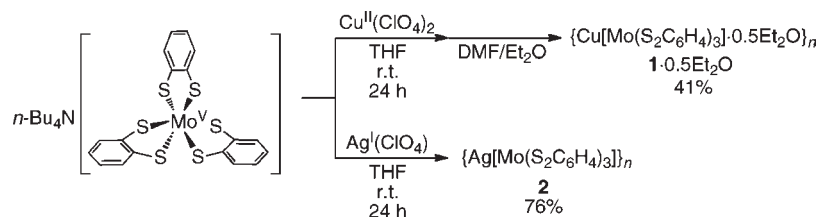
Scheme 1. Synthetic Scheme for $1 \cdot 0.5\text{Et}_2\text{O}$ and **2**

Figure 1. Crystallographically independent units of (a) $1 \cdot 0.5\text{Et}_2\text{O}$ and (b) **2** with thermal ellipsoid plots for Mo (blue), Cu (brown), Ag (black), and S (yellow) (50% probability). Solvent molecules (Et_2O) for $1 \cdot 0.5\text{Et}_2\text{O}$ and hydrogen atoms are omitted for clarity.

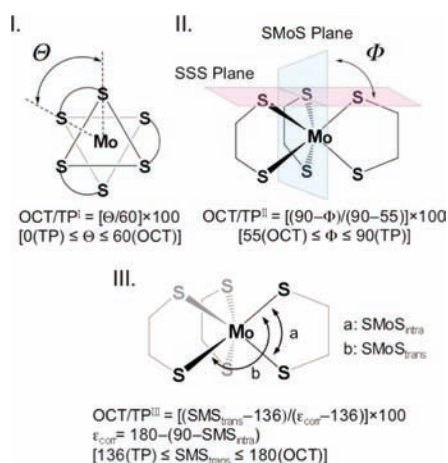
Table 2. Selected Bond Distances (Å) for $1 \cdot 0.5\text{Et}_2\text{O}$ and **2**

	$1 \cdot 0.5\text{Et}_2\text{O}$	2	$[\text{Mo}^{\text{VI}}(\text{bdt})_3]^{0a}$	$[\text{Mo}^{\text{V}}(\text{bdt})_3]^{-b}$	$[\text{Mo}^{\text{IV}}(\text{bdt})_3]^{2-b}$
Mo(1)–S(1) [L1]	2.3882(8)	2.3661(7)	2.370(2)	2.3882(8)	2.3952(14)
Mo(1)–S(2) [L1]	2.4031(9)	2.3680(4)	2.360(2)	2.4020(8)	2.3981(12)
Mo(1)–S(3) [L2]	2.3717(10)	2.4091(4)	2.371(2)	2.3702(7)	2.3940(12)
Mo(1)–S(4) [L2]	2.4277(8)	2.4148(5)		2.3778(8)	
Mo(1)–S(5) [L3]	2.4291(9)	2.4181(5)		2.3999(8)	
Mo(1)–S(6) [L3]	2.4297(10)	2.4014(5)		2.3785(7)	
Mo(2)–S(7) [L4]	2.4102(8)				
Mo(2)–S(8) [L4]	2.3703(10)				
Mo(2)–S(9) [L5]	2.4582(9)				
Mo(2)–S(10) [L5]	2.3748(9)				
Mo(2)–S(11) [L6]	2.3911(9)				
Mo(2)–S(12) [L6]	2.4310(10)				
average	2.4071(9)	2.3963(5)	2.367(2)	2.3861(8)	2.396(1)
Cu(1)–S(1)	2.3113(8)	Ag(1)–S(3)	2.6857(5)		
Cu(1)–S(6)	2.3502(9)	Ag(1)–S(4)	2.6510(5)		
Cu(1)–S(7)	2.4060(10)	Ag(1)–S(5)	2.5950(6)		
Cu(1)–S(9)	2.3276(9)	Ag(1)–S(6)	2.6837(6)		
Cu(2)–S(4)	2.3145(9)				
Cu(2)–S(5)	2.3387(9)				
Cu(2)–S(10)	2.3614(10)				
Cu(2)–S(12)	2.3552(9)				
average	2.3456(9)	2.6539(6)			

^aReference 12b. ^bReference 12c.

that can be stored in air for extended periods of time without decomposition. In contrast to the high solubility of

$n\text{-Bu}_4\text{N}[\text{Mo}^{\text{V}}(\text{bdt})_3]$ in polar organic and halogenated solvents such as acetone, THF, dichloromethane, and chloroform, that of

Chart 1. Definitions of OCT/TP^I, OCT/TP^{II}, and OCT/TP^{III}(%)**Table 3.** Geometrical Parameters for **1**·0.5Et₂O and **2**

		OCT/TP ^I	OCT/TP ^{II}	OCT/TP ^{III}
[(Ph ₃ P) ₂ N] ₂ [Mo ^{IV} (bdt) ₃] ^a		41.3	42.8	47.9
(Et ₃ NH) ₂ [Mo ^{IV} (bdtCl ₂) ₃] ^b		0.0	0.0	3.4
[(Ph ₃ P) ₂ N][Mo ^V (bdt) ₃] ^a		58.6	59.9	70.4
(<i>n</i> -Bu ₄ N)[Mo ^V (bdt) ₃] ^c		55.8	58.0	64.0
[Mo ^{VI} (bdt) ₃] ^d		0.0	0.0	1.0
1 ·0.5Et ₂ O	Mo1	55.7	72.6	77.7
	Mo2	68.3	57.7	54.0
2	Mo	63.0	65.5	61.4

^a Reference 12c. ^b Reference 12e. ^c Reference 12a. ^d Reference 12b.

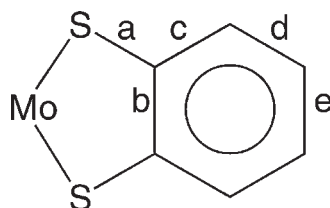
1·0.5Et₂O is quite low, indicating the stability of the polymer structure of **1**·0.5Et₂O. However, the complex **1**·0.5Et₂O can be dissolved in highly polar organic solvents such as CH₃CN, DMF, and DMSO. On the other hand, the similar reaction of *n*-Bu₄N[Mo^V(bdt)₃] with a colorless THF solution of Ag^IClO₄ at RT for 24 h resulted in the formation of **2** in 76% yield as a black powder, which also can be stored in air over an extended time period without any decomposition. In contrast to the cases of *n*-Bu₄N[Mo^V(bdt)₃] and **1**·0.5Et₂O, complex **2** is insoluble in all organic solvents and water, suggesting a rigid coordination network for **2**.

Crystal Structures of 1·0.5Et₂O and 2. The crystallographically independent units of **1**·0.5Et₂O and **2** are shown in Figure 1, and their selected bond distances are summarized in Table 2 together with those of previously reported mononuclear complexes [Mo(bdt)₃]ⁿ (*n* = 0, −1, and −2).^{12b,c} In the crystal structure of **1**·0.5Et₂O, two crystallographically independent Mo and Cu atoms are found. It is well-known that tris(dithiolene)molybdenum complexes can adopt both octahedral (OCT) and trigonal-prismatic (TP) structures.¹² According to the classification of Beswick et al.,^{4a} the coordination geometries largely depend upon the mixed nature of the coordinating dithiolene ligands, crystal packing affected by counter-cations, and oxidation numbers of the metal centers. The estimated geometrical parameters of OCT/TP(%), which are defined in

Chart 1, for **1**·0.5Et₂O and **2** together with those of related mononuclear complexes are summarized in Table 3. From the comparison of OCT/TP(%) parameters of referenced mononuclear complexes, the neutral complex ([Mo^{VI}(bdt)₃]⁰) tends to possess high TP-character, which has been reasonably explained by molecular orbital calculations.^{7d,12a–12c,19} Furthermore, the monoanionic complex ([Mo^V(bdt)₃][−]) has higher OCT-character rather than that of the dianionic complex ([Mo^{IV}(bdt)₃]^{2−}) regardless of the different counter-cations. In both cases of **1**·0.5Et₂O and **2**, it was shown that the geometries of the Mo center are pseudo-octahedral. The OCT-characters are slightly larger in **1**·0.5Et₂O and **2** than in those of the starting material *n*-Bu₄N[Mo^V(bdt)₃] and other referenced complexes, predominantly because of the presence of additional coordination of bdt to Cu and Ag ions for **1**·0.5Et₂O and **2**, respectively (vide infra).

The Mo–S bond distances of **1**·0.5Et₂O (2.4071(9) Å) and **2** (2.3963(5) Å) are slightly longer than those of [Mo^V(bdt)₃][−] (2.3861(8) Å) and [Mo^{VI}(bdt)₃]⁰ (2.367(2) Å), and close to that of [Mo^{IV}(bdt)₃]^{2−} (2.396(1) Å). In comparing the Mo–S bond distances in the series [Mo(bdt)₃]ⁿ (*n* = 0, −1, and −2), the molybdenum ion having a higher oxidation state forms a shorter coordination bond with the sulfur atom, interpreted in terms of strong electron donation from the sulfur atom to the molybdenum center with an electron-deficient higher oxidation state. However, complexes **1**·0.5Et₂O and **2** have longer Mo–S bond distances compared with related mononuclear complexes; they cannot be explained only based on the oxidation state of the Mo center. In the similar dithiolene palladium complex [Pd^{II}(mnt){O₂S₂C₂(CN)₂}]^{2−} (mnt = 1,2-dicyano-1,2-ethylenedithiolato, O₂S₂C₂(CN)₂ = 1,2-dicyano-ethylene-1-thiolato-2-sulfinato) and its complex with additional Ag^I ions {AgPd(mnt)(O₂S₂C₂(CN)₂)₂}^{2−}, which was reported by Munakata and co-workers,^{13a} bond distances between palladium and sulfur belonging to the mnt in {AgPd(mnt)(O₂S₂C₂(CN)₂)₂}^{2−} are elongated compared with that in [Pd^{II}(mnt){O₂S₂C₂(CN)₂}]^{2−}. Such bond elongation can be understood by the decreased electron density on sulfur and weakened coordination bond to the palladium center. Similarly, such longer Mo–S bond distances in **1**·0.5Et₂O and **2** should also be a consequence of the decrease in the electron density on sulfur atoms induced by directly connected Cu and Ag cations.

For more detailed information about electronic structural assignments for **1**·0.5Et₂O and **2**, comparison of structural parameters with those of previously reported complexes [Mo(S₂C₆H₄)₃]ⁿ (*n* = 0, −1, and −2) have been made.^{12b,c} The average S–C bond distances in **1**·0.5Et₂O (1.757(4) Å) and **2** (1.753(2) Å) summarized in Table 4 are obviously longer than that of [Mo^{VI}(S₂C₆H₄)₃]⁰ (1.727 Å) and close to that of [(Ph₃P)₂N][Mo^V(S₂C₆H₄)₃] (1.749 Å). In the case of [Mo^{VI}(S₂C₆H₄)₃]⁰, partial oxidation of the dithiolato ligand to dithiobenzoquinonato⁰ or dithiobenzosemiquinonato[−] is found based on the shorter S–C bond distances.^{12b} However, the S–C(a) bond in **1**·0.5Et₂O and **2** can be described as a single bond, and the oxidation states of the molybdenum center should be lower than Mo^{VI}. Such a S–C bond elongation character with changes in the molybdenum oxidation states from Mo^{VI} to Mo^{IV} is also corroborated by the difference of the C–C bond lengths in the aromatic ring. The suggestions described above are also supported by the fact that the bond distances of C–C(b) and C–C(e) in **1**·0.5Et₂O (1.395(5) and 1.379(8) Å) and **2** (1.397(3) and 1.386(4) Å) are shorter than those of

Table 4. Bond Distances (Å) of S₂C₆H₄ Moieties in 1·0.5Et₂O and 2

		Å					
		a	b	c	d	e	
[(Ph ₃ P) ₂ N] ₂ [Mo ^{IV} (S ₂ C ₆ H ₄) ₃] ^a	average	1.759	1.396	1.405	1.390	1.377	
[(Ph ₃ P) ₂ N][Mo ^V (S ₂ C ₆ H ₄) ₃] ^a	average	1.749	1.392	1.402	1.378	1.385	
[Mo ^{VI} (S ₂ C ₆ H ₄) ₃] ^b	average	1.727	1.411	1.399	1.359	1.406	
1·0.5Et ₂ O	L1	1.736(4)	1.401(5)	1.402(6)	1.389(6)	1.387(7)	
		1.760(4)		1.401(5)	1.390(7)		
	L2	1.758(3)	1.403(5)	1.402(5)	1.386(6)	1.381(6)	
		1.756(3)		1.404(5)	1.388(6)		
	L3	1.768(4)	1.401(5)	1.401(6)	1.387(6)	1.392(7)	
		1.760(4)		1.404(5)	1.381(6)		
	L4	1.763(3)	1.389(5)	1.410(5)	1.389(6)	1.384(7)	
		1.760(3)		1.398(5)	1.375(6)		
	L5	1.759(4)	1.385(6)	1.413(6)	1.402(7)	1.385(9)	
		1.754(4)		1.402(6)	1.379(7)		
	L6	1.748(4)	1.392(6)	1.408(6)	1.384(9)	1.347(9)	
		1.759(4)		1.406(6)	1.386(7)		
		average	1.757(4)	1.395(5)	1.404(6)	1.386(7)	1.379(8)
	2	L1	1.736(2)	1.392(3)	1.403(4)	1.381(4)	1.383(4)
1.737(2)				1.408(3)	1.384(4)		
L2		1.760(2)	1.402(3)	1.400(2)	1.377(3)	1.391(3)	
		1.760(2)		1.398(3)	1.386(3)		
L3		1.766(2)	1.396(3)	1.401(3)	1.384(3)	1.385(4)	
		1.756(2)		1.403(3)	1.380(3)		
		average	1.753(2)	1.397(3)	1.402(3)	1.382(3)	1.386(4)

^a Reference 12c. ^b Reference 12b.

[Mo^{VI}(S₂C₆H₄)₃]⁰ (1.411 and 1.460 Å), and the C–C(d) bond distances of 1·0.5Et₂O (1.386(7) Å) and 2 (1.382(3) Å) are longer than that of [Mo^{VI}(S₂C₆H₄)₃]⁰ (1.359 Å). Briefly, bond elongation in C–C(b), C–C(c), and C–C(e) together with bond shortening at C–C(d) indicates that partial oxidation of the dithiolato ligand to dithiobenzoquinonato⁰ or dithiobenzoquinonato[–] is not obtained in 1·0.5Et₂O and 2. Thus, it is concluded that the S₂C₆H₄^{2–} moieties in 1·0.5Et₂O and 2 can be best described as *o*-benzenedithiolato dianion (bdt^{2–}), and the oxidation states of the molybdenum center are reasonably assigned as Mo^V, leading to the electronic structures of [Mo^V(S₂C₆H₄)₃][–] moieties in 1·0.5Et₂O and 2 as [Mo^V(bdt)₃][–].

In addition, the Cu atom with distorted tetrahedral geometry in 1·0.5Et₂O is coordinated by four S atoms of bdt, which is the most common geometry for monovalent copper ions.²⁰ Each Cu atom in 1·0.5Et₂O is shared by two [Mo^V(bdt)₃][–] units with an average Cu–S bond distance of 2.3456(9) Å. Similarly, the Ag atoms in 2 are also coordinated

by four S atoms with distorted tetrahedral geometry, which is the most common geometry for monovalent silver ions, with an average value for the Ag–S bond distances of 2.6539(6) Å. The Ag atom in 2 is shared by three [Mo^V(bdt)₃][–] units, leading to the formation of a denser structure than in the case of 1·0.5Et₂O.

From the structural features described above, descriptions of the total electronic structures of 1·0.5Et₂O and 2 are consequently written as {M'[Mo^V(bdt)₃]}_n (M' = Cu^I and Ag^I). It should be noted that the divalent copper in the starting material was reduced to monovalent copper during the reaction. The formation of 1 is most probably interpreted in terms of the redox-selective complexation reaction of [Mo^V(bdt)₃][–] with Cu^I (eq 2), which was formed by a one-electron redox reaction between the half amount of Cu^{II} and [Mo^V(bdt)₃][–] to afford [Mo^{VI}(bdt)₃]⁰ as a byproduct (eq 1). This reaction mechanism can be supported by the positive redox potential of E_{1/2}(Cu^I/Cu^{II}) = 0.73 V (vs Ag/Ag⁺) in CH₃CN solution compared with E_{1/2}([Mo^V(bdt)₃][–]/

$[\text{Mo}^{\text{VI}}(\text{bdt})_3]^0 = 0.00 \text{ V}$ in CH_3CN solution (vide infra). In fact, the complex $\mathbf{1} \cdot 0.5\text{Et}_2\text{O}$ could be synthesized by the similar reaction of $n\text{-Bu}_4\text{N}[\text{Mo}^{\text{V}}(\text{bdt})_3]$ with $\text{Cu}^{\text{I}}(\text{CH}_3\text{CN})_4\text{ClO}_4$ in higher yield (81%) than the case of $\text{Cu}^{\text{II}}(\text{ClO}_4)_2 \cdot 6\text{H}_2\text{O}$, and could not be obtained by the reaction between $[\text{Mo}^{\text{VI}}(\text{bdt})_3]^0$ and Cu^{II} . On the other hand, in the case of $\mathbf{2}$, the complexation reaction between $[\text{Mo}^{\text{V}}(\text{bdt})_3]^-$ and Ag^{I} proceeded to

afford $\mathbf{2}$ without any redox process, a fact that is also supported by the redox potentials of $[\text{Mo}^{\text{V}}(\text{bdt})_3]^- / [\text{Mo}^{\text{VI}}(\text{bdt})_3]^0$ versus Ag/Ag^+ .

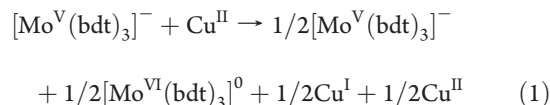
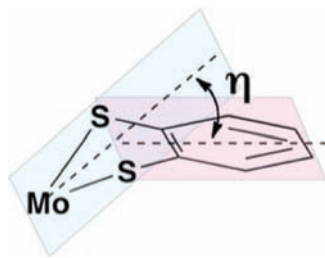
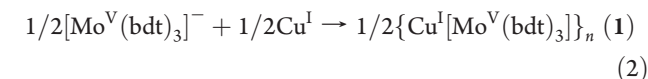


Table 5. Bending Angles (η) of bdt^{2-} in $\mathbf{1} \cdot 0.5\text{Et}_2\text{O}$ and $\mathbf{2}$



	η/deg
<i>n</i> -Bu ₄ N[Mo ^V (bdt) ₃] ^a	
S(1)Mo(1)S(2)/S(1)C(1)C(2)S(2)	6.94
S(3)Mo(1)S(4)/S(3)C(7)C(8)S(4)	6.68
S(5)Mo(1)S(6)/S(5)C(13)C(14)S(6)	9.88
average	7.83
$\mathbf{1} \cdot 0.5\text{Et}_2\text{O}$	
L1	19.09
L2	5.45
L3	9.09
L4	22.79
L5	1.82
L6	7.88
average	11.02
$\mathbf{2}$	
L1	3.14
L2	29.78
L3	26.89
average	19.94

^aReference 12a.



It is noteworthy that the remarkable influence caused by the complexation with Cu^{I} and/or Ag^{I} ions is found especially with bdt moieties. The ligand distortion angles (η) between the SMoS and the SCCS planes in bdt are summarized in Table 5 along with that of $n\text{-Bu}_4\text{N}[\text{Mo}^{\text{V}}(\text{bdt})_3]$.^{12a} It is well-known that the distortion of mononuclear dithiolene complexes is closely linked to the improved overlap between the ligand π_v and the metal d_{z^2} orbitals (second-order Jahn–Teller distortion).²¹ The bdt bends moderately in $n\text{-Bu}_4\text{N}[\text{Mo}^{\text{V}}(\text{bdt})_3]$ at an average angle of $\eta = 7.83^\circ$. It becomes much larger in the case of $\mathbf{1} \cdot 0.5\text{Et}_2\text{O}$ ($\eta(\text{average}) = 11.02^\circ$) and $\mathbf{2}$ ($\eta(\text{average}) = 19.94^\circ$) probably because of the steric repulsion between neighboring $[\text{Mo}^{\text{V}}(\text{bdt})_3]^-$ units. In the complex $\mathbf{1} \cdot 0.5\text{Et}_2\text{O}$, most of the bdt lock in a gear–mesh fashion with neighboring $[\text{Mo}^{\text{V}}(\text{bdt})_3]^-$ units, but some of them, such as L1 and L4, are bent with larger distortion angles ($\eta = 19.09$ and 22.79°) than the others because of the steric repulsion. Meanwhile, the distortion angles of L2 and L3 ($\eta = 29.78$ and 26.89°) in $\mathbf{2}$, which are shared by Mo^{V} and Ag^{I} ions, are larger than that of L1 ($\eta = 3.14^\circ$), which is independent of Ag^{I} ions. Such larger angles for L2 and L3 occur as the result of the π – π interaction of the aromatic ring with neighboring bdt (vide infra). This characteristic distortion indicates the flexibility of the $[\text{Mo}^{\text{V}}(\text{bdt})_3]^-$ moiety, which permits the formation of assemblies by changing its structure so as to energetically minimize a lattice in response to the steric repulsion of the bulky $[\text{Mo}^{\text{V}}(\text{bdt})_3]^-$ unit and size differences between the Cu^{I} (0.91 Å) and the Ag^{I} (1.29 Å) ions.²² These characteristic properties of $\mathbf{1} \cdot 0.5\text{Et}_2\text{O}$ and $\mathbf{2}$ are summarized in Figure 2, showing changes of coordination geometries around the Mo atoms and bdt distortion between $\mathbf{1} \cdot 0.5\text{Et}_2\text{O}$, $\mathbf{2}$, and the starting material $n\text{-Bu}_4\text{N}[\text{Mo}^{\text{V}}(\text{bdt})_3]$.

One-Dimensional (1-D) Chain Structures of $\mathbf{1} \cdot 0.5\text{Et}_2\text{O}$ and $\mathbf{2}$. The unit structures of $\mathbf{1} \cdot 0.5\text{Et}_2\text{O}$ and $\mathbf{2}$ described above are commonly connected by the sulfur atoms of bdt to form 1-D chain structures along the *b*-axis as shown in Figure 3. In the case of $\mathbf{1} \cdot 0.5\text{Et}_2\text{O}$, $\Delta\Lambda$ -chirality around the pseudo-octahedral Mo^{V}

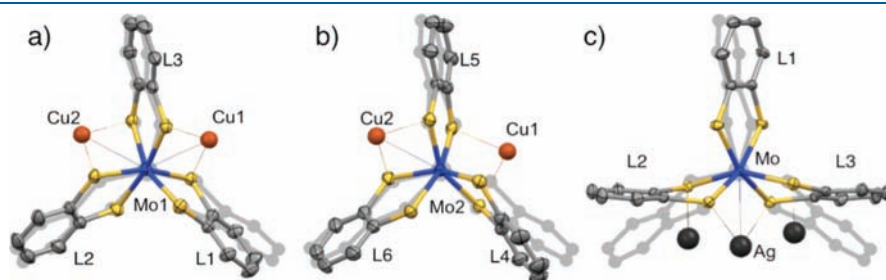


Figure 2. (a) Structure of the $\{\text{Cu}^{\text{I}}_2[\text{Mo}^{\text{V}}(\text{bdt})_3]\}_3$ moiety around the Mo1 atom and (b) around the Mo2 atom in $\mathbf{1} \cdot 0.5\text{Et}_2\text{O}$. (c) Structure of the $\{\text{Ag}^{\text{I}}_3[\text{Mo}^{\text{V}}(\text{bdt})_3]\}_3$ moiety in $\mathbf{2}$. Structure of $n\text{-Bu}_4\text{N}[\text{Mo}^{\text{V}}(\text{bdt})_3]$ without the ammonium countercation is shown by the shadowgraph in each case.^{12a} Hydrogen atoms are omitted for clarity.

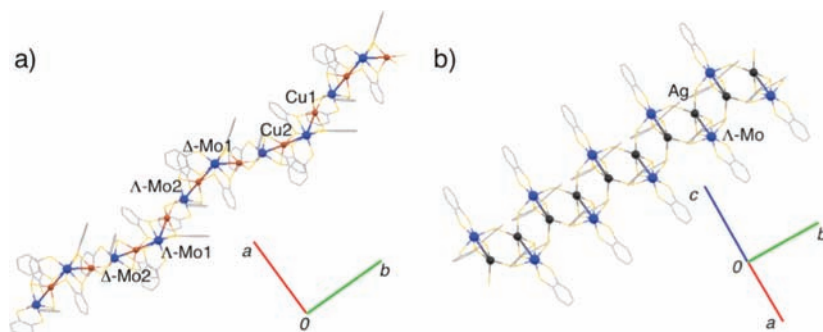


Figure 3. Chain structures of (a) $1 \cdot 0.5\text{Et}_2\text{O}$ and (b) **2**. Hydrogen atoms are omitted for clarity.

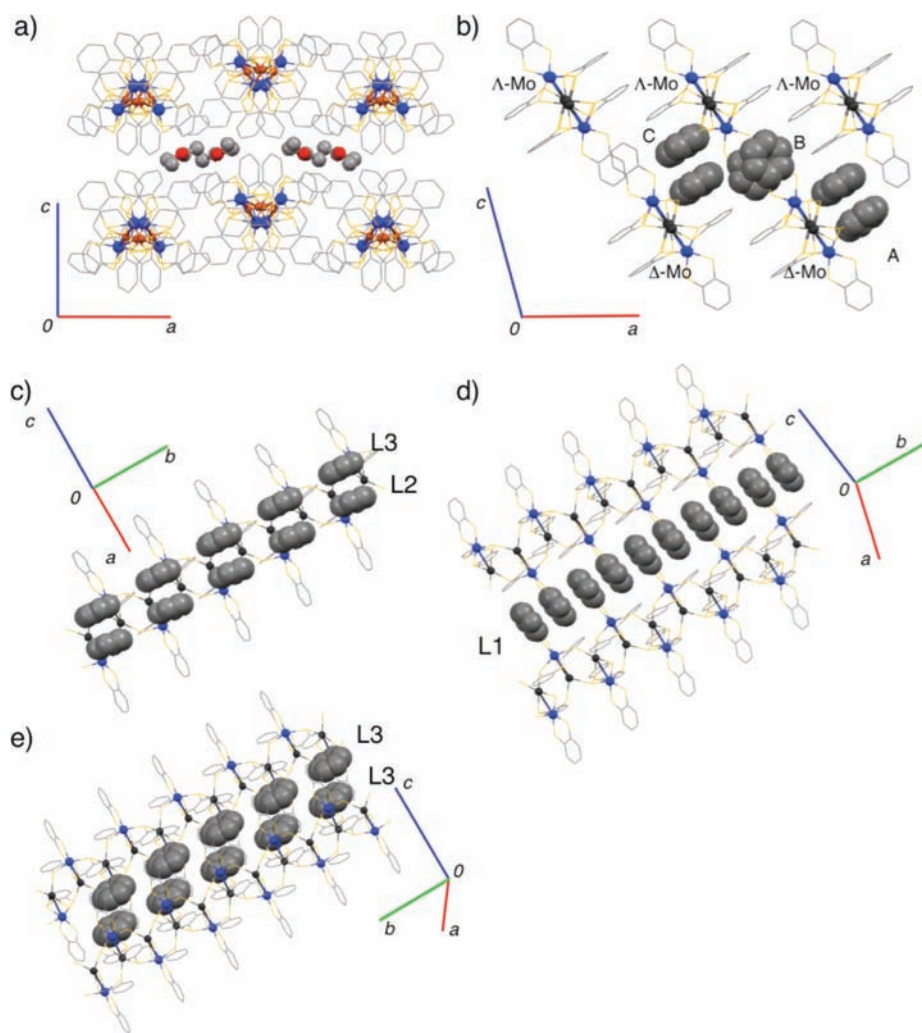


Figure 4. Assembled structures of (a) $1 \cdot 0.5\text{Et}_2\text{O}$ and (b) **2** projected along the b -axis. Et_2O molecules in $1 \cdot 0.5\text{Et}_2\text{O}$ are drawn as ball- and stick models in (a). (c) Intrachain π - π interaction (A), and interchain π - π interactions (d) (B) and (e) (C) of **2**. Bdt rings involved with π - π interactions are drawn as space-filling models in (b–e).

center produces a racemic mixture in the chain (Figure 3a). Furthermore, Et_2O molecules are introduced between the chains in $1 \cdot 0.5\text{Et}_2\text{O}$ (Figure 4a). In the case of **2**, Mo^{V} and Ag^{I} atoms lie in a zigzag manner along the b -axis to construct the 1-D chain structure (Figure 3b). In contrast to the case of $1 \cdot 0.5\text{Et}_2\text{O}$, $\Delta\Lambda$ -chirality around the Mo^{V} center in **2** is unified in the chain. The

isomeric chain is alternately stacked along the c -axis. Interestingly, an intrachain (A) π - π stacking structure is formed between neighboring L2 and L3. Furthermore, L1 and L3 also form two types of interchain π - π stacking interactions (B and C) with each other (Figures 4b, 4c, 4d, and 4e). The distances between the closest carbon atoms in the aromatic rings are 3.595,

Table 6. UV-vis Spectroscopic Data of **1**, **2**, and *n*-Bu₄N[Mo^V(bdt)₃] in Solution and in the Solid State

complex	conc. (M)	λ , nm (ϵ , M ⁻¹ cm ⁻¹)				solvent	ref.
<i>n</i> -Bu ₄ N[Mo ^V (bdt) ₃]	1.05 × 10 ⁻³	408 (10700)	482 (8580)	609 (4750)	691 (4100)	CH ₃ CN	this work
		414 (14500)	614 (6300)	693 (5900)		THF	ref. ^{12a}
1	1.05 × 10 ⁻³	430 (11200)	614 (4580)	721 (4760)		CH ₃ CN	this work
	1.05 × 10 ⁻⁴	412 (11500)	479 (9080)	614 (4820)	709 (4620)	CH ₃ CN	this work
	1.05 × 10 ⁻⁵	409 (11500)	482 (8380)	615 (4670)	696 (4300)	CH ₃ CN	this work
<i>n</i> -Bu ₄ N[Mo ^V (bdt) ₃] ^a	solid	420.5	493.5	625	749		this work
1 ^a	solid	487.5	510.5	657.5			this work
2 ^a	solid	435.5	532	680			this work

^a Measured for KBr pellets.

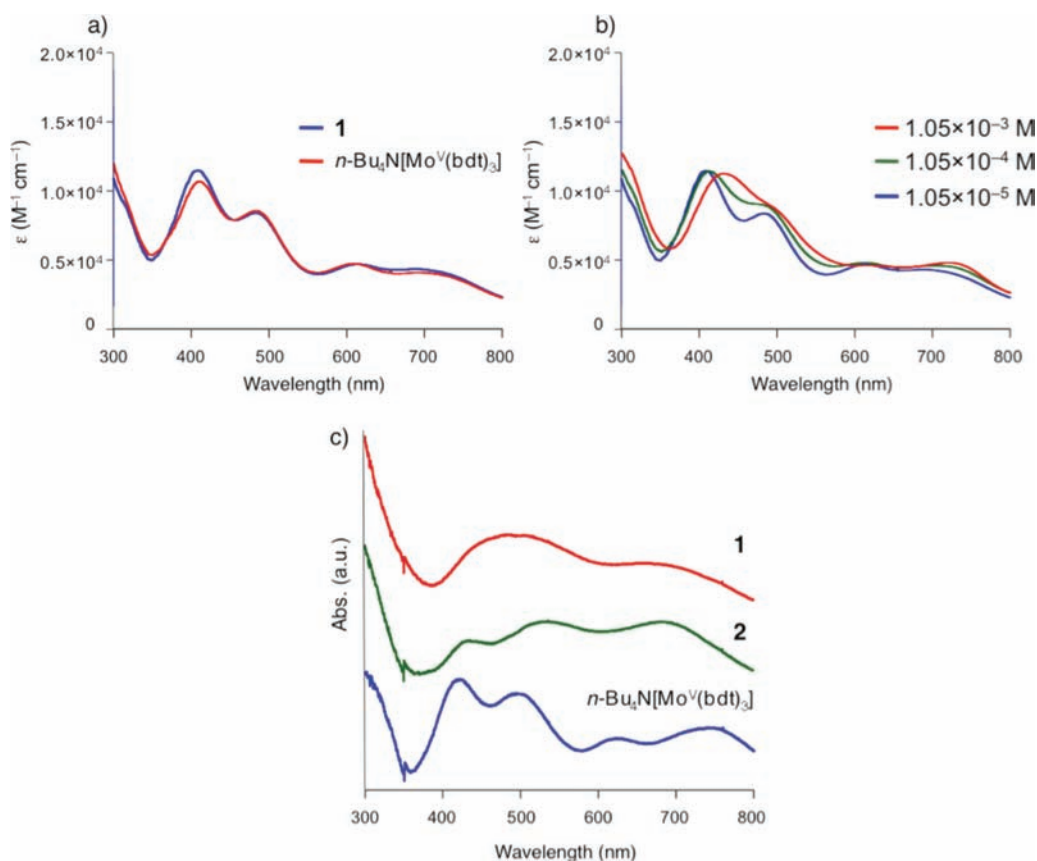


Figure 5. (a) UV-vis spectra of **1** (blue line) and *n*-Bu₄N[Mo^V(bdt)₃] (red line) in CH₃CN solution at RT (1.05 × 10⁻³ M). (b) Concentration-dependent UV-vis spectra of **1** in CH₃CN solution at RT (1.05 × 10⁻³ M (red line), 1.05 × 10⁻⁴ M (green line), 1.05 × 10⁻⁵ M (blue line)). (c) UV-vis spectra of **1** (red line), **2** (green line), and *n*-Bu₄N[Mo^V(bdt)₃] (blue line) in the solid state using KBr pellets.

3.464, and 3.402 Å in (A), (B), and (C), respectively. It is strongly suggested that the dimensionality of the assembly should be much higher than a simple one-dimension as a result of intra- and interchain interactions in **2**. Such strong crystal packing with higher dimensionality is reflected in the insolubility of **2** in organic solvents and water after the formation of the assembly, in contrast to the case of **1**·0.5Et₂O, which can be dissolved in polar solvents such as CH₃CN, DMF, and DMSO.

UV-vis Spectra of 1·0.5Et₂O and 2. To the best of our knowledge, most coordination polymers are insoluble after construction, and examples of soluble coordination polymers are quite rare.²³

However, as described above, complex **1**·0.5Et₂O is remarkably soluble in polar organic solvents, and such solubility naturally prompted us to investigate the spectroscopic properties of **1** in solution. Complex **1** gives a dark brown color in CH₃CN solution at 1.05 × 10⁻³ M, different from the dark purple color in the solid state, the intense color of which is reflected in the high molar extinction coefficients of the four bands in the visible region. The pattern of these bands at 1.05 × 10⁻⁵ M is quite similar to that obtained for *n*-Bu₄N[Mo^V(bdt)₃] (Figure 5a). The UV-vis spectra of **1** at different concentrations (1.05 × 10⁻³–1.05 × 10⁻⁵ M) in CH₃CN are shown in Figure 5b, and relevant data for **1** are listed in Table 6

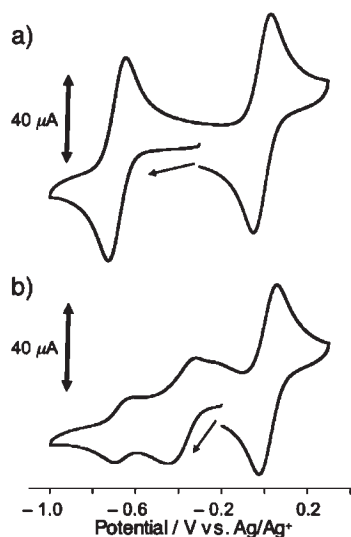


Figure 6. Cyclic voltammograms of (a) $n\text{-Bu}_4\text{N}[\text{Mo}^{\text{V}}(\text{bdt})_3]$ and (b) **1** in CH_3CN (1 mM) with 0.1 M $n\text{-Bu}_4\text{NPF}_6$ as supporting electrolyte at RT. Conditions: 500 mV/s scan rates; glassy carbon working electrode; redox potentials are referenced versus Ag/Ag^+ .

together with data for $n\text{-Bu}_4\text{N}[\text{Mo}^{\text{V}}(\text{bdt})_3]$. A red shift of the absorption bands, especially in the shorter wavelength region (400–600 nm), was observed with increase in concentration from 1.05×10^{-5} M to 1.05×10^{-3} M. On the other hand, the UV–vis spectrum of **1** in the solid state was measured using a KBr pellet (Figure 5c). The dark brown solution of **1** in CH_3CN at 1.05×10^{-3} M changed to olive green with decrease in the concentration to 1.05×10^{-5} M. It is notable that the shape of the spectrum in solution of **1** at higher concentrations, such as 1.05×10^{-3} M, is very similar to that in the solid state. Such concentration-dependent spectral behavior should be considered in relation to the complexation of the Cu^{I} ion and $[\text{Mo}^{\text{V}}(\text{bdt})_3]^-$ unit in solution. On the basis of such concentration-dependent spectral changes of **1**, the existence of oligomeric species with a higher degree of association at higher concentration can be suggested for highly polar solvents such as CH_3CN , DMF, and DMSO. In addition, the fact that complex **1** was crystallized by layering Et_2O onto the DMF solution of **1** suggests that the coordination polymer is reassembled by addition of a poor solvent. In contrast, the UV–vis spectrum of **2** in solution could not be measured because of the insolubility of **2** in organic solvents and water. However, the structures of the absorption bands of **2** in the solid state are quite different from that observed for $n\text{-Bu}_4\text{N}[\text{Mo}^{\text{V}}(\text{bdt})_3]$, and it is qualitatively indicated that the electronic structure of the chromophore is significantly affected by the formation of the polymeric structure with Ag^{I} in **2**.

Redox Property of 1. The cyclic voltammogram of **1** in CH_3CN (1 mM) is shown in Figure 6b together with that of $n\text{-Bu}_4\text{N}[\text{Mo}^{\text{V}}(\text{bdt})_3]$ in Figure 6a. Two quasi-reversible couples are observed at -0.68 ($E_{1/2}^{\text{Red}}$) and 0.00 V ($E_{1/2}^{\text{Ox}}$) for $n\text{-Bu}_4\text{N}[\text{Mo}^{\text{V}}(\text{bdt})_3]$, which correspond to two one-electron redox processes of $[\text{Mo}^{\text{IV}}(\text{bdt})_3]^{2-}/[\text{Mo}^{\text{V}}(\text{bdt})_3]^-$ and $[\text{Mo}^{\text{V}}(\text{bdt})_3]^-/[\text{Mo}^{\text{VI}}(\text{bdt})_3]^0$.^{12a,d,24} Comparatively, the cyclic voltammogram of **1** displays three quasi-reversible waves at -0.65 ($E_{1/2}^{\text{Red}}$), -0.38 ($E_{1/2}^{\text{Red}}$), and 0.02 V ($E_{1/2}^{\text{Ox}}$) respectively. The potentials of $E_{1/2}^{\text{Red}}$ and $E_{1/2}^{\text{Ox}}$ in **1** are quite similar to those of $E_{1/2}^{\text{Red}}$ and $E_{1/2}^{\text{Ox}}$ in $n\text{-Bu}_4\text{N}[\text{Mo}^{\text{V}}(\text{bdt})_3]$.

The redox process at $E_{1/2}^{\text{Red}}$ is characteristic for **1**, and is not obtained for starting material $n\text{-Bu}_4\text{N}[\text{Mo}^{\text{V}}(\text{bdt})_3]$. Based on the similarity of $E_{1/2}^{\text{Ox}}$ in **1** and $E_{1/2}^{\text{Ox}}$ in $n\text{-Bu}_4\text{N}[\text{Mo}^{\text{V}}(\text{bdt})_3]$, the electrochemical process at $E_{1/2}^{\text{Ox}}$ of **1** presumably corresponds to the molybdenum-centered oxidation process of **1** or oligomeric species constructed from $[\text{Mo}^{\text{V}}(\text{bdt})_3]^-$ and Cu^{I} ions to produce the oxidized species $[\text{Mo}^{\text{VI}}(\text{bdt})_3]^0$ or $\{\text{Cu}^{\text{I}}[\text{Mo}^{\text{VI}}(\text{bdt})_3]\}^+$ ($[\text{1}]^+$) and/or its valence tautomer $\{\text{Cu}^{\text{II}}[\text{Mo}^{\text{V}}(\text{bdt})_3]\}^+$. Considering that the assemblies constructed from $[\text{Mo}^{\text{VI}}(\text{bdt})_3]^0$ and Cu^{I} or $[\text{Mo}^{\text{V}}(\text{bdt})_3]^-$ and Cu^{II} ions were not obtained during the synthesis of **1**, such an intermediate should be dissociated within a certain time scale. On the other hand, the peak currents of the two quasi-reversible waves for $E_{1/2}^{\text{Red}}$ and $E_{1/2}^{\text{Red}}$ are much smaller than those of $n\text{-Bu}_4\text{N}[\text{Mo}^{\text{V}}(\text{bdt})_3]$ (almost 30% for $E_{1/2}^{\text{Red}}$ and 70% for $E_{1/2}^{\text{Red}}$ compared with $E_{1/2}^{\text{Ox}}$ process of **1**). It is notable that the redox process at $E_{1/2}^{\text{Red}}$ of **1** was obtained at a similar potential region to $E_{1/2}^{\text{Red}}$ of $n\text{-Bu}_4\text{N}[\text{Mo}^{\text{V}}(\text{bdt})_3]$. The electrochemical process at $E_{1/2}^{\text{Red}}$ of **1** probably corresponds to the reduction process of the $[\text{Mo}^{\text{V}}(\text{bdt})_3]^-$ unit, which might be generated by the dissociative equilibrium of the oligomeric species consisting of $[\text{Mo}^{\text{V}}(\text{bdt})_3]^-$ and Cu^{I} ion. Moreover, the process at $E_{1/2}^{\text{Red}}$ in the voltammogram of **1** could be assigned to the reduction process of oligomeric species of Cu^{I} and $[\text{Mo}^{\text{V}}(\text{bdt})_3]^-$ units. The presence of such oligomeric species in CH_3CN solution at 1 mM is supported by concentration-dependent UV–vis spectra, as discussed previously. The positively shifted potential of the $E_{1/2}^{\text{Red}}$ process compared with that of $E_{1/2}^{\text{Red}}$ can be ascribed to the increased electron-accepting nature of the Mo^{V} center influenced by the S-coordinating Cu^{I} cations in the oligomeric structure. Although the ratio of the current values in **1**, especially for $E_{1/2}^{\text{Red}}$ and $E_{1/2}^{\text{Red}}$, might be considerable in relation to the dissociation constants of **1** to $[\text{Mo}^{\text{V}}(\text{bdt})_3]^-$ or oligomeric species in CH_3CN solution, it is indicative that each process is not straightforward, and the exact behavior of the species remains unclear, because chains (oligomers/polymers) could also be formed in solution.

CONCLUSIONS

Coordination polymers **1** and **2** constructed from $[\text{Mo}^{\text{V}}(\text{bdt})_3]^-$ units and Cu^{I} and/or Ag^{I} ions were successfully synthesized by the reactions of $n\text{-Bu}_4\text{N}[\text{Mo}^{\text{V}}(\text{bdt})_3]$ and equivalent perchlorate salts of Cu^{II} and/or Ag^{I} ions. X-ray crystallographic analyses revealed differences in the 1-D polymeric structures, and interchain interactions. For complex **1** having an infinite chain structure in the solid state, the existence of an oligomeric structure at higher concentration was strongly suggested by UV–vis spectroscopic analysis and electrochemical studies. In the case of **2**, an assembled structure with a higher dimensionality than that of **1** is obtained, and that reflects the insolubility of **2** in different types of solvents. The presented results suggest that the assembly utilizing metal-dithiolato complexes such as $[\text{M}(\text{dithiolato})_m]^{n-}$ as metalloligand with additional metal ions can be a useful approach, enabling modulation not only of the assembled structure in the solid state but also of the electrochemical properties of heteromultinuclear assembled systems in the solution state. In other words, metal-dependent and redox-selective properties demonstrate the potential of $[\text{M}(\text{dithiolato})_m]^{n-}$ units as functional metalloligands with a controllable assembled structure that may lead to functionality such as electrocatalytic behavior, and strongly indicate the importance of a systematic understanding of this chemistry utilizing different types of $[\text{M}(\text{dithiolato})_m]^{n-}$, additional metal ions, and dithiolato ligands.

■ ASSOCIATED CONTENT

S Supporting Information. Temperature-dependent χ_M plots of $1 \cdot 0.5\text{Et}_2\text{O}$, **2**, and $n\text{-Bu}_4\text{N}[\text{Mo}^{\text{V}}(\text{bdt})_3]$, UV-vis spectral change with addition of CH_3CN solution of $\text{Cu}^{\text{I}}(\text{CH}_3\text{CN})_4\text{ClO}_4$ to the CH_3CN solution of $n\text{-Bu}_4\text{N}[\text{Mo}^{\text{V}}(\text{bdt})_3]$, cyclic voltammograms of **1** and $n\text{-Bu}_4\text{N}[\text{Mo}^{\text{V}}(\text{bdt})_3]$, and ESI-MS spectrum of **1**. X-ray crystallographic data for $1 \cdot 0.5\text{Et}_2\text{O}$ and **2** in cif format. This material is available free of charge via the Internet at <http://pubs.acs.org>.

■ AUTHOR INFORMATION

Corresponding Author

*E-mail: mkato@sci.hokudai.ac.jp. Phone: +81-11-706-3817. Fax: +81-11-706-3447.

■ ACKNOWLEDGMENT

The authors are grateful to Prof. Yukio Hinatsu, Prof. Makoto Wakeshima, Prof. Takayoshi Nakamura, Prof. Shin-ichiro Noro, and Dr. Toru Endo (Hokkaido Univ.) for great support and discussions in magnetic measurements. This work was supported by Elements Science and Technology Project “Nano-hybridized Precious-metal-free Catalysts for Chemical Energy Conversion” and a Grants-in-Aid for Scientific Research for Priority Area “Coordination Programming” (Area No. 2107) from the Ministry of Education, Culture, Sports, Science and Technology (MEXT), Japan.

■ REFERENCES

- (1) (a) Drain, C. M.; Varotto, A.; Radivojevic, I. *Chem. Rev.* **2009**, *109*, 1630–1658. (b) Swiggers, G. F.; Malefetse, T. J. *Chem. Rev.* **2000**, *100*, 3483–3537. (c) Rosen, B. M.; Wilson, C. J.; Wilson, D. A.; Peterca, M.; Imam, M. R.; Percec, V. *Chem. Rev.* **2009**, *109*, 6275–6540. (d) Niu, Z.; Gibson, H. W. *Chem. Rev.* **2009**, *109*, 6024–6046. (e) Beletskaya, I.; Tyurin, V. S.; Tsvivadze, A. Y.; Guillard, R.; Stern, C. *Chem. Rev.* **2009**, *109*, 1659–1713. (f) Eryazici, I.; Moorefield, C. N.; Newkome, G. R. *Chem. Rev.* **2008**, *108*, 1834–1895. (g) Zangrando, E.; Casanova, M.; Alessio, E. *Chem. Rev.* **2008**, *108*, 4979–5013. (h) Giacalone, F.; Martin, N. *Chem. Rev.* **2006**, *106*, 5136–5190.
- (2) (a) Fujita, M.; Tominaga, M.; Hori, A.; Therrien, B. *Acc. Chem. Res.* **2005**, *38*, 369–378. (b) Ganguly, R.; Sreenivasulu, B.; Vittal, J. J. *Coord. Chem. Rev.* **2008**, *252*, 1027–1050. (c) Dalgarno, S. J.; Power, N. P.; Atwood, J. L. *Coord. Chem. Rev.* **2008**, *252*, 825–841. (d) Maji, T. K.; Kitagawa, S. *Pure Appl. Chem.* **2007**, *79*, 2155–2177. (e) Kitagawa, S.; Matsuda, R. *Coord. Chem. Rev.* **2007**, *251*, 2490–2509. (f) Kitagawa, S.; Uemura, K. *Chem. Soc. Rev.* **2005**, *34*, 109–119. (g) Kitagawa, S.; Masaoka, S. *Coord. Chem. Rev.* **2003**, *246*, 73–88. (h) O’Keeffe, M.; Peskov, M. A.; Ramsden, S. J.; Yaghi, O. M. *Acc. Chem. Res.* **2008**, *41*, 1782–1789. (i) Halder, G. J.; Kepert, C. J.; Moubaraki, B.; Murray, K. S.; Cashion, J. D. *Science* **2002**, *298*, 1762–1765. (j) Taylor, J. M.; Mah, R. K.; Moudrakovski, I. L.; Ratcliffe, C. I.; Vaidhyanathan, R.; Shimizu, G. K. H. *J. Am. Chem. Soc.* **2010**, *132*, 14055–14057. (k) Tong, M.-L.; Chen, X.-M.; Batten, S. R. *J. Am. Chem. Soc.* **2003**, *125*, 16170–16171.
- (3) (a) Schrauzer, G. N. *Acc. Chem. Res.* **1969**, *2*, 72–80. (b) *Dithiolen Chemistry: Synthesis, Properties, and Applications*; Stiefel, E. I., Ed.; John Wiley & Sons: New York, 2004; Vol. 52. (c) Schrauzer, G. N.; Mayweg, V. *J. Am. Chem. Soc.* **1962**, *84*, 3221–3221. (d) Davison, A.; Edelstein, N.; Holm, R. H.; Maki, A. H. *J. Am. Chem. Soc.* **1963**, *85*, 3049–3050. (e) Davison, A.; Edelstein, N.; Holm, R. H.; Maki, A. H. *Inorg. Chem.* **1963**, *2*, 1227–1232. (f) Davison, A.; Edelstein, N.; Holm, R. H.; Maki, A. H. *J. Am. Chem. Soc.* **1963**, *85*, 2029–2030. (g) Eisenberg, R. *Prog. Inorg. Chem.* **1970**, *12*, 295–369. (h) Gray, H. B.; Billig, E. *J. Am. Chem. Soc.* **1963**, *85*, 2019–2020. (i) McCleverty, J. A. *Prog. Inorg. Chem.*

1968, *10*, 49–221. (j) Mahadevan, C. J. *Crystallogr. Spectrosc. Res.* **1986**, *16*, 347–416. (k) Williams, J. M.; Wang, H. H.; Emge, T. J.; Geiser, U.; Beno, M. A.; Leung, P. C. W.; Carlson, K. D.; Thorn, R. J.; Schultz, A. J.; Whangbo, M. H. *Prog. Inorg. Chem.* **1987**, *35*, 51–218. (l) Fourmigue, M. *Coord. Chem. Rev.* **1998**, *178–180*, 823–864. (m) Nomura, M.; Cauchy, T.; Fourmigue, M. *Coord. Chem. Rev.* **2010**, *254*, 1406–1418.

(4) (a) Beswick, C. L.; Schulman, J. M.; Stiefel, E. I. *Prog. Inorg. Chem.* **2004**, *52*, 55–110. (b) Johnson, M. K. *Prog. Inorg. Chem.* **2004**, *52*, 213–266.

(5) (a) Kirk, M. L.; McNaughton, R. L.; Helton, M. E. *Prog. Inorg. Chem.* **2004**, *52*, 111–212. (b) Rauchfuss, T. B. *Prog. Inorg. Chem.* **2004**, *52*, 1–54. (c) Wang, K. *Prog. Inorg. Chem.* **2004**, *52*, 267–314. (d) Sellmann, D.; Sutter, J. *Prog. Inorg. Chem.* **2004**, *52*, 585–681.

(6) (a) Faulmann, C.; Cassoux, P. *Prog. Inorg. Chem.* **2004**, *52*, 399–489. (b) Cassoux, P.; Valade, L.; Kobayashi, H.; Kobayashi, A.; Clark, R. A.; Underhill, A. E. *Coord. Chem. Rev.* **1991**, *110*, 115–160.

(7) (a) Helton, M. E.; Gruhn, N. E.; McNaughton, R. L.; Kirk, M. L. *Inorg. Chem.* **2000**, *39*, 2273–2278. (b) Stiefel, E. I. *Pure Appl. Chem.* **1998**, *70*, 889–896. (c) Helton, M. E.; Gebhart, N. L.; Davies, E. S.; McMaster, J.; Garner, C. D.; Kirk, M. L. *J. Am. Chem. Soc.* **2001**, *123*, 10389–10390. (d) Stiefel, E. I.; Eisenberg, R.; Rosenberg, R. C.; Gray, H. B. *J. Am. Chem. Soc.* **1966**, *88*, 2956–2966. (e) Wang, K.; McConnachie, J. M.; Stiefel, E. I. *Inorg. Chem.* **1999**, *38*, 4334–4341. (f) Harmer, M. A.; Halbert, T. R.; Pan, W. H.; Coyle, C. L.; Cohen, S. A.; Stiefel, E. I. *Polyhedron* **1986**, *5*, 341–347. (g) Ward, M. D.; McCleverty, J. A. *J. Chem. Soc., Dalton Trans.* **2002**, 275–288. (h) Ray, K.; Petrenko, T.; Wiegardt, K.; Neese, F. *Dalton Trans.* **2007**, 1552–1566.

(8) (a) Battaglia, R.; Henning, R.; Dinh-Ngoc, B.; Schlamann, W.; Kisch, H. *J. Mol. Catal.* **1983**, *21*, 239–253. (b) Katakis, D. F.; Mitsopoulou, C.; Konstantatos, J.; Vrachnou, E.; Falaras, P. *J. Photochem. Photobiol., A* **1992**, *68*, 375–388. (c) Katakis, D.; Mitsopoulou, C.; Vrachnou, E. *J. Photochem. Photobiol., A* **1994**, *81*, 103–106. (d) Paw, W.; Cummings, S. D.; Mansour, M. A.; Connick, W. B.; Geiger, D. K.; Eisenberg, R. *Coord. Chem. Rev.* **1998**, *171*, 125–150. (e) Hissler, M.; McGarrath, J. E.; Connick, W. B.; Geiger, D. K.; Cummings, S. D.; Eisenberg, R. *Coord. Chem. Rev.* **2000**, *208*, 115–137.

(9) (a) Chen, C. T.; Liao, S. Y.; Lin, K. J.; Lai, L. L. *Adv. Mater.* **1998**, *10*, 334–338. (b) Winter, C. S.; Oliver, S. N.; Rush, J. D.; Hill, C. A. S.; Underhill, A. E. *J. Appl. Phys.* **1992**, *71*, 512–514. (c) Hill, C. A. S.; Underhill, A. E.; Winter, C. S.; Oliver, S. N.; Rush, J. D. *Spec. Publ. - R. Soc. Chem.* **1991**, *91*, 217–222. (d) Winter, C. S.; Hill, C. A. S.; Underhill, A. E. *Appl. Phys. Lett.* **1991**, *58*, 107–109. (e) Underhill, A. E.; Hill, C. A. S. *Mol. Cryst. Liq. Cryst. Sci. Technol., Sect. A* **1992**, *217*, 7–12. (f) Winter, C. S.; Oliver, S. N.; Manning, R. J.; Rush, J. D.; Hill, C. A. S.; Underhill, A. E. *J. Mater. Chem.* **1992**, *2*, 443–447. (g) Hill, C. A. S.; Charlton, A.; Underhill, A. E.; Malik, K. M. A.; Hursthouse, M. B.; Karaulov, A. I.; Oliver, S. N.; Kershaw, S. V. *J. Chem. Soc., Dalton Trans.* **1995**, 587–594. (h) Cummings, S. D.; Cheng, L.-T.; Eisenberg, R. *Chem. Mater.* **1997**, *9*, 440–450.

(10) (a) Abbott, A. P.; Jenkins, P. R.; Khan, N. S. *J. Chem. Soc., Chem. Commun.* **1994**, 1935–1936. (b) Mueller-Westerhoff, U. T.; Vance, B.; Yoon, D. I. *Tetrahedron* **1991**, *47*, 909–932.

(11) (a) Pilato, R. S.; Eriksen, M. K. A.; Greaney, M. A.; Stiefel, E. I.; Goswami, S.; Kilpatrick, L.; Spiro, T. G.; Taylor, E. C.; Rheingold, A. L. *J. Am. Chem. Soc.* **1991**, *113*, 9372–9374. (b) Subramanian, P.; Burgmayer, S.; Richards, S.; Szalai, V.; Spiro, T. G. *Inorg. Chem.* **1990**, *29*, 3849–3853. (c) Soricelli, C. L.; Szalai, V. A.; Burgmayer, S. J. N. *J. Am. Chem. Soc.* **1991**, *113*, 9877–9878. (d) Kilpatrick, L.; Rajagopalan, K. V.; Hilton, J.; Bastian, N. R.; Stiefel, E. I.; Pilato, R. S.; Spiro, T. G. *Biochemistry* **1995**, *34*, 3032–3039. (e) Rees, D. C.; Hu, Y.; Kisker, C.; Schindelin, H. *J. Chem. Soc., Dalton Trans.* **1997**, 3909–3914. (f) Burgmayer, S. J. N. *Prog. Inorg. Chem.* **2004**, *52*, 491–537. (g) Kisker, C.; Schindelin, H.; Rees, D. C. *Annu. Rev. Biochem.* **1997**, *66*, 233–267. (h) Rudolph, M. J.; Wuebbens, M. M.; Rajagopalan, K. V.; Schindelin, H. *Nat. Struct. Biol.* **2001**, *8*, 42–46. (i) Stiefel, E. I. *J. Chem. Soc., Dalton Trans.* **1997**, 3915–3924. (j) Thapper, A.; Lorber, C.; Fryxellius, J.; Behrens, A.; Nordlander, E. *J. Inorg. Biochem.* **2000**, *79*, 67–74. (k) Basu, P.; Stolz, J. F.; Smith, M. T. *Curr. Sci.* **2003**, *84*, 1412–1418. (l) Enemark, J. H.; Cooney, J. J. A.; Wang, J.-J.; Holm, R. H. *Chem. Rev.* **2004**,

104, 1175–1200. (m) Enemark, J. H.; Garner, C. D. *J. Biol. Inorg. Chem.* **1997**, *2*, 817–822. (n) Johnson, M. K.; Garton, S. D.; Oku, H. *JBIC, J. Biol. Inorg. Chem.* **1997**, *2*, 797–803. (o) Romao, M. J.; Rosch, N.; Huber, R. *JBIC, J. Biol. Inorg. Chem.* **1997**, *2*, 782–785. (p) Sugimoto, H.; Tsukube, H. *Chem. Soc. Rev.* **2008**, *37*, 2609–2619. (q) Sugimoto, H.; Suyama, K.; Sugimoto, K.; Miyake, H.; Takahashi, I.; Hirota, S.; Itoh, S. *Inorg. Chem.* **2008**, *47*, 10150–10157. (r) Sugimoto, H.; Tatamoto, S.; Suyama, K.; Miyake, H.; Itoh, S.; Dong, C.; Yang, J.; Kirk, M. L. *Inorg. Chem.* **2009**, *48*, 10581–10590.

(12) (a) Cervilla, A.; Llopis, E.; Marco, D.; Perez, F. *Inorg. Chem.* **2001**, *40*, 6525–6528. (b) Cowie, M.; Bennett, M. J. *Inorg. Chem.* **1976**, *15*, 1584–1589. (c) Isfort, C. S.; Pape, T.; Hahn, F. E. *Eur. J. Inorg. Chem.* **2005**, 2607–2611. (d) Kapre Ruta, R.; Bothe, E.; Weyhermuller, T.; DeBeer George, S.; Wieghardt, K. *Inorg. Chem.* **2007**, *46*, 5642–5650. (e) Sugimoto, H.; Furukawa, Y.; Tarumizu, M.; Miyake, H.; Tanaka, K.; Tsukube, H. *Eur. J. Inorg. Chem.* **2005**, 3088–3092.

(13) (a) Sugimoto, K.; Kuroda-Sowa, T.; Maekawa, M.; Munakata, M. *Bull. Chem. Soc. Jpn.* **2000**, *73*, 391–394. (b) Ebihara, M.; Tsuchiya, M.; Yamada, M.; Tokoro, K.; Kawamura, T. *Inorg. Chim. Acta* **1995**, *231*, 35–43.

(14) (a) Hemmerich, P.; Sigwart, C. *Experientia* **1963**, *19*, 488–489. (b) Csoregh, I.; Kierkegaard, P.; Norrestam, R. *Acta Crystallogr.* **1975**, *B31*, 314–317. (c) Kitagawa, S.; Munakata, M. *Inorg. Chem.* **1981**, *20*, 2261–2267. (d) Deivaraj, T. C.; Vittal, J. J. *J. Chem. Soc., Dalton Trans.* **2001**, 322–328.

(15) Burla, M. C.; Caliendo, R.; Camalli, M.; Carrozzini, B.; Cascarano, G. L.; De Caro, L.; Giacovazzo, C.; Polidori, G.; Spagna, R. *J. Appl. Crystallogr.* **2005**, *38*, 381–388.

(16) Beurskens, P. T.; Admiraal, G.; Beurskens, G.; de Gelder, R.; Garcia-Granda, S.; Gould, R. O.; Israel, R.; Smits, J. M. M. *DIRDIF-99*; University of Nijmegen: Nijmegen, The Netherlands, 1999.

(17) *CrystalStructure 3.8.2*, Crystal Structure Analysis Package; Rigaku and Rigaku/MSC: The Woodlands, TX, 2000–2006.

(18) Sheldrick, G.. *SHELX-97, Program for Crystal Structure Solution and the Refinement of Crystal Structures*; Institut für Anorganische Chemie der Universität Göttingen: Göttingen, Germany, 1997.

(19) (a) Schrauzer, G. N.; Mayweg, V. P. *J. Am. Chem. Soc.* **1966**, *88*, 3235–3242. (b) Cervilla, A.; Ramirez, J. A.; Llopis, E.; Palanca, P. *Inorg. Chem.* **1993**, *32*, 2085–2091.

(20) Greenwood, N. N.; Earnshaw, A. *Chemistry of the Elements*; Pergamon: Oxford, 1984; p 1542.

(21) Campbell, S.; Harris, S. *Inorg. Chem.* **1996**, *35*, 3285–3288.

(22) (a) Pauling, L. C. *The Nature of the Chemical Bond and the Structure of Molecules and Crystals*, 3rd ed.; Cornell University Press: Ithaca, NY, 1960; p 644. (b) Pauling, L. *J. Chem. Educ.* **1992**, *69*, 519–521.

(23) (a) Friese, V. A.; Kurth, D. G. *Coord. Chem. Rev.* **2008**, *252*, 199–211. (b) Ikeda, T.; Higuchi, M.; Kurth, D. G. *J. Am. Chem. Soc.* **2009**, *131*, 9158–9159. (c) Han, F. S.; Higuchi, M.; Kurth, D. G. *J. Am. Chem. Soc.* **2008**, *130*, 2073–2081. (d) Gasnier, A.; Barbe, J.-M.; Bucher, C.; Duboc, C.; Moutet, J.-C.; Saint-Aman, E.; Terech, P.; Royal, G. *Inorg. Chem.* **2010**, *49*, 2592–2599. (e) Gasnier, A.; Barbe, J.-M.; Bucher, C.; Denat, F.; Moutet, J.-C.; Saint-Aman, E.; Terech, P.; Royal, G. *Inorg. Chem.* **2008**, *47*, 1862–1864. (f) Larionova, J.; Guari, Y.; Sayegh, H.; Guerin, C. *Inorg. Chim. Acta* **2007**, *360*, 3829–3836. (g) Jiang, P.; Huang, W.; Li, J.; Zhuang, D.; Shi, J. *J. Mater. Chem.* **2008**, *18*, 3688–3693.

(24) (a) Cervilla, A.; Perez-Pla, F.; Llopis, E. *Chem. Commun.* **2001**, 2332–2333. (b) Cervilla, A.; Perez-Pla, F.; Llopis, E.; Piles, M. *Inorg. Chem.* **2006**, *45*, 7357–7366. (c) Perez-Pla, F.; Cervilla, A.; Piles, M.; Llopis, E. *Inorg. Chem.* **2009**, *48*, 8559–8568. (d) Cervilla, A.; Perez-Pla, F.; Llopis, E.; Piles, M. *Inorg. Chem.* **2005**, *44*, 4106–4108.